

ARTICLE

Received 22 Oct 2013 | Accepted 10 Feb 2014 | Published 3 Mar 2014

DOI: 10.1038/ncomms4419

Trunk cleavage is essential for *Drosophila* terminal patterning and can occur independently of Torso-like

Michelle A. Henstridge^{1,*}, Travis K. Johnson^{1,2,*}, Coral G. Warr¹ & James C. Whisstock^{2,3}

Terminal patterning in *Drosophila* is governed by a localized interaction between the Torso kinase (Tor) and its ligand Trunk (Trk). Currently, it is proposed that Trk must be cleaved in order to bind Tor, and that these proteolytic events are controlled by secretion of Torso-like (Tsl) only at the embryo poles. However, controversy surrounds these ideas since neither cleaved Trk nor a protease that functions in terminal patterning have been identified. Here we show that Trk is cleaved multiple times *in vivo* and that these proteolytic events are essential for its function. Unexpectedly, however, the Trk cleavage patterns we observe are unaltered in *tsl*-null mutants. One explanation for these data is that the influence of Tsl on localized Trk cleavage at the embryo poles is subtle and cannot be readily detected. Alternatively, we favour a scenario where Tsl functions post proteolytic processing of Trk to control localized terminal patterning.

¹School of Biological Sciences, Monash University, Clayton, Victoria 3800, Australia. ²Department of Biochemistry and Molecular Biology, Monash University, Clayton, Victoria 3800, Australia. ³Australian Research Council Centre of Excellence in Advanced Molecular Imaging, Monash University, Clayton, Victoria 3800, Australia. * These authors contributed equally to the work. Correspondence and requests for materials should be addressed to C.G.W. (email: coral.warr@monash.edu) or to J.C.W. (email: james.whisstock@monash.edu).

Patterning of the *Drosophila* embryo depends on spatial cues provided by maternal gene products and has served as a model paradigm for studying the localized activation of important developmental signalling pathways such as Toll and receptor tyrosine kinase signalling. In *Drosophila*, terminal patterning is achieved by localized activation of the Torso (Tor) receptor tyrosine kinase. The proposed ligand for Tor is Trunk (Trk), a protein that is most similar to the Noggin-like branch of the cysteine-knot superfamily^{1,2}. Other notable cysteine knot-like family members in *Drosophila* include Spätzle (Spz), the growth factor that binds the Toll receptor, thus initiating dorsoventral patterning^{3,4}. In this system, the Spz ligand is generated through the actions of a complex extracellular proteolytic cascade⁴. Given that Trk has the same cysteine knot-like fold as Spz⁵, it has been previously suggested that Trk might be cleaved in order to bind and activate the Tor receptor⁵.

In support of these ideas, Casali and Casanova⁶ used the Easter protein signal peptide to express shortened Trk variants (lacking either 76 or 127 amino acids in the amino terminus) in the extracellular region between the oocyte cytoplasmic membrane and vitelline membrane (the perivitelline (PV) space). These constructs were able to ubiquitously activate Tor signalling and bypass other known maternal factors, albeit inefficiently. In addition to suggesting a requirement for Trk proteolytic processing, these studies also strongly implicate Trk as the Tor

ligand in terminal patterning. Further, it is notable that a second Tor ligand, prothoracicotropic hormone, lacks a Trk-like N-terminal region¹ and can constitutively activate Tor in the absence of other factors⁷.

Despite these findings, a major question in terminal patterning remains unsolved—how is Tor signalling localized to the embryonic poles? The homogeneous distribution of *tor* messenger RNA in embryos⁸, in addition to several lines of genetic evidence^{9–11} suggests that Tor is present ubiquitously on the embryo plasma membrane. Similarly, Trk is also produced in the oocyte and, while its trafficking remains to be understood, it is suggested that it is secreted into the PV space^{5,11}. Currently, the only known localized factor in the terminal patterning pathway is Torso-like (Tsl)—a membrane attack complex/perforin-like (MACPF) protein that is secreted from specialized follicle cells at the anterior and posterior ends of the oocyte^{10,12,13}. Homozygous *tsl*-mutant females produce embryos that lack all terminal structures, characteristic of the terminal-class genes. Importantly, however, ectopic expression of Tsl from all follicle cells produces ubiquitous Tor signalling, resulting in expanded terminal regions at the expense of the central segments^{10,12}. Given its specific localization at the poles, and the likely requirement for Trk cleavage, it has been proposed that Tsl permits a protease to cleave Trk into its active form only at the embryo poles⁶. However, in contrast to the dorsoventral

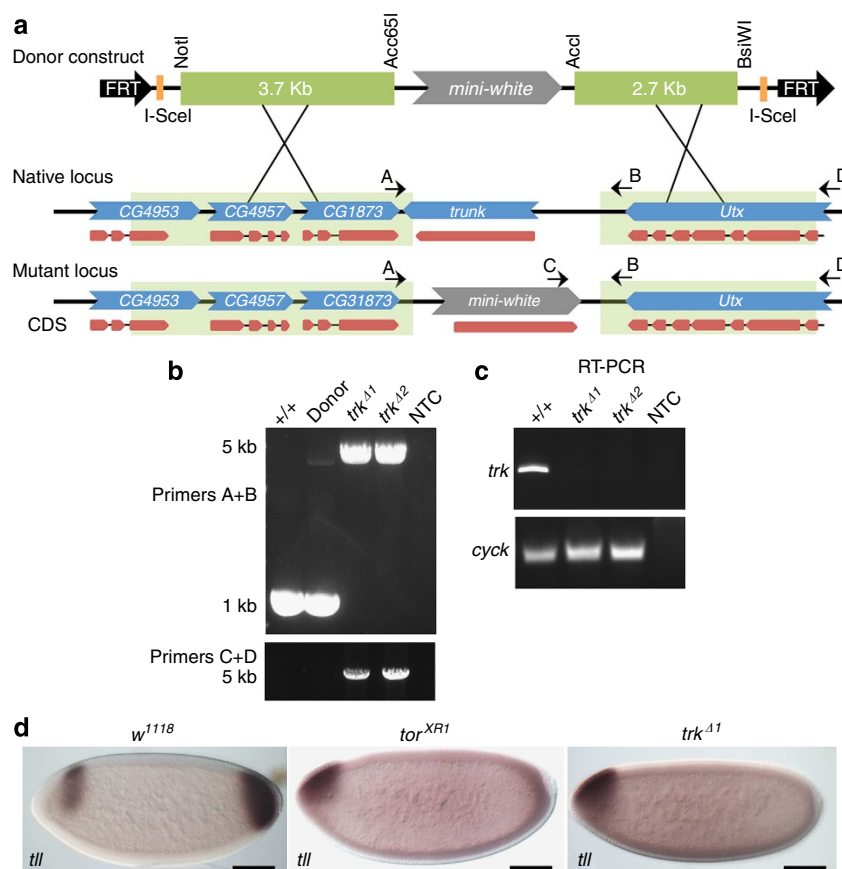


Figure 1 | Generation of a *trk*-null mutant via ends-out gene targeting. (a) Targeting scheme for the removal of the *trk* coding sequence using ends-out gene replacement. The donor construct was generated by cloning 2.7 kb of upstream and 3.7 kb of downstream flanking sequence. (b) Verification of *trk*-targeted events. Primers A and B span the targeted region and amplify 5 kb when *trk* has been replaced by the white gene from pw25 (1 kb amplicon results from untargeted locus). Primers C and D amplify 5 kb only when targeting events have occurred. (c) RT-PCR confirms lack of *trk* transcripts in two *trk*-null mutant lines (400 bp amplicon is present in wild-type control, the *cycK*-positive control amplicon is 145 bp, NTC, no template control). (d) RNA *in situ* hybridization of early embryos with a probe to *tailless* (*tll*), a zygotic gene that is transcribed in response to Tor signalling. Embryos laid by *trk*^{Δ1} females display defective *tll* expression identical to that observed in embryos maternally lacking *tor* (*tor*^{XRT}), indicating a failure to specify terminal fate. Scale bars, 100 μm. Anterior is positioned to the left.

patterning system, where a major cascade of proteases and regulatory serpins are known and characterized¹⁴, to date no protease required for terminal patterning has been found, nor has a cleaved Trk species been identified.

Here we provide direct evidence of Trk proteolytic processing in protein extracts from early embryos, finding that it is cleaved multiple times. We also show that this cleavage is necessary for its function in the activation of Tor. Finally, we test the long-standing idea that Tsl is required for Trk cleavage. Surprisingly, we find that Trk cleavage can take place in the absence of Tsl. One explanation for these data is that most Trk cleavage events are independent of Tsl, and that a small amount of Tsl-dependent changes in Trk cleavage occurring only at the embryo poles cannot be detected. Alternatively, we argue that our data favour a model where Tsl functions post proteolytic processing of Trk to control localized terminal patterning.

Results

Trk is cleaved multiple times. To investigate Trk activation, we set out to ascertain whether Trk cleavage is required for terminal patterning. We were unable to generate satisfactory antibodies for Trk; hence, we generated transgenic flies carrying various N- and C-terminally tagged forms of Trk. To ensure further studies were performed on a functional Trk protein, we first determined which of the tagged proteins could successfully rescue *trk*-null mutants. Since available stocks carrying *trk*-mutant alleles are likely hypomorphic and/or have additional genetic mutations, ends-out gene replacement was used to generate a *trk*-null mutant allele (*trk*^Δ) in which the entire coding region is removed (Fig. 1). *trk*^Δ homozygotes are viable but females are sterile, laying embryos that fail to specify terminal cell fate (Fig. 1).

Several combinations of large (fluorescent protein) and small (epitope) tags revealed the N terminus of Trk to be insensitive to tagging (Fig. 2a). While Trk function was lost upon C-terminal fusion with GFP, addition of smaller epitopes to the C-terminus had no functional consequences (Fig. 2). Expression of one functional C-terminally tagged Trk protein, HA:Trk:Myc, was detectable in embryo samples by immunoblotting for the Myc tag (35 kDa, Fig. 3a). Importantly, concentration of the fusion protein in embryo extracts via immunoprecipitation revealed the presence of at least six C-terminal Trk fragments ranging from 10–35 kDa (Fig. 3b). This is consistent with the idea that Trk may undergo several cleavage events. We note that although this construct has both N-terminal hemagglutinin (HA) and C-terminal Myc tags, only the full-length fusion protein was detected with anti-HA; no smaller N-terminal Trk fragments could be detected after immunoprecipitation (Fig. 3c). As we have only been able to detect full-length N-terminally tagged protein, it is possible that the N-terminal region, once removed, is rapidly degraded.

Trk cleavage is required for terminal patterning. Given these data, we were then in a position to investigate whether Trk cleavage is required for its function. Previously, Casanova *et al.*⁵ predicted a possible cleavage site at R76-S77 via local sequence similarity to a cleavage sequence present in complement C3. We further noted that a dibasic motif (K75 and R76 in *D. melanogaster* Trk) is conserved across Trk proteins from different *Drosophila* species, as well as in other insect Trk proteins, consistent with a recognition sequence for a target protease (Fig. 4a). Because Trk shares significant sequence similarity and domain architecture to the mammalian growth factor Noggin (ref. 1 and Fig. 4b), we analysed the Trk sequence with respect to the X-ray crystal structure of Noggin². This revealed that K75-R76 likely maps to a mobile (disordered in

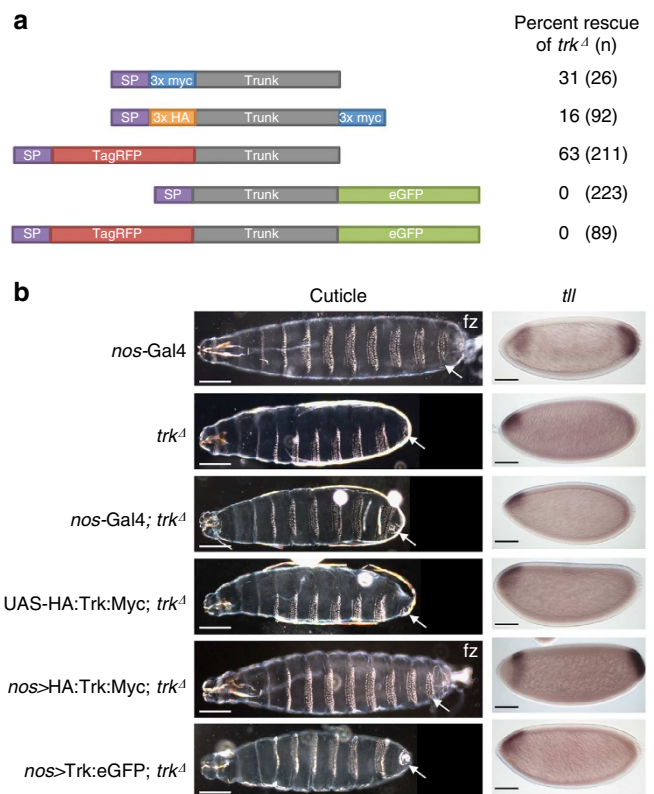


Figure 2 | Rescue of the *trk*^Δ terminal phenotype by expression of a tagged form of Trk. (a) Schematic representation of tagged Trk proteins that were tested for their ability to rescue the *trk*^Δ-mutant phenotype. The N-terminal signal sequence of Trk (purple box, SP) was used in all cases. The relative ability of the individual fusion proteins to rescue the *trk*^Δ-mutant phenotype is indicated. (b) The wild-type control (*nos-Gal4*) first-instar larval cuticle shows the presence of normal terminal structures, including abdominal segments posterior to A7 (arrowed) and the filzkörper (fz) and normal *tailless* (*tll*) expression. The *trk*^Δ cuticle lacks abdominal segments posterior to A7 and filzkörper, and shows an altered *tll* expression pattern with complete loss at the posterior (typical of a terminal-class mutant). We found that for individual embryos, maternal expression of Trk with *nos-Gal4* gave either complete rescue (wild-type phenotype) or no rescue at all (*trk*^Δ phenotype), representative examples of each are shown (HA:Trk:Myc rescues, Trk:eGFP does not). Scale bars, 100 μ m. Anterior is to the left and maternal genotypes are as indicated. For each experiment at least two independent transgenic Trk lines were tested.

electron density) exposed loop that could be accessible by a target protease (Fig. 4c). To test this, we performed an *in vivo* alanine scan of Trk across residues H71-P82, using the rescue of terminal patterning in *trk*^Δ mutants as an assay for function (Fig. 4d). Both the K75A and R76A mutations abolished Trk function (Fig. 4d,e). In contrast, Trk proteins containing mutations N- or C-terminal of these two amino-acid positions retained function (Fig. 4d).

Having demonstrated the functional importance of the K75-R76 sequence, we investigated whether the K75A and R76A mutations impacted on Trk cleavage. Strikingly, the Trk_{K75A,R76A} mutation resulted in the loss of two C-terminal Trk fragments (Fig. 3b), thus identifying K75 and R76 as key determinants of specificity for Trk cleavage. Further, together with our earlier findings, these data demonstrate that abolishing a Trk cleavage event is directly associated with loss of Trk function. Importantly, for the first time, these data also demonstrate an ability to detect changes in Trk cleavage patterns *in vivo*.

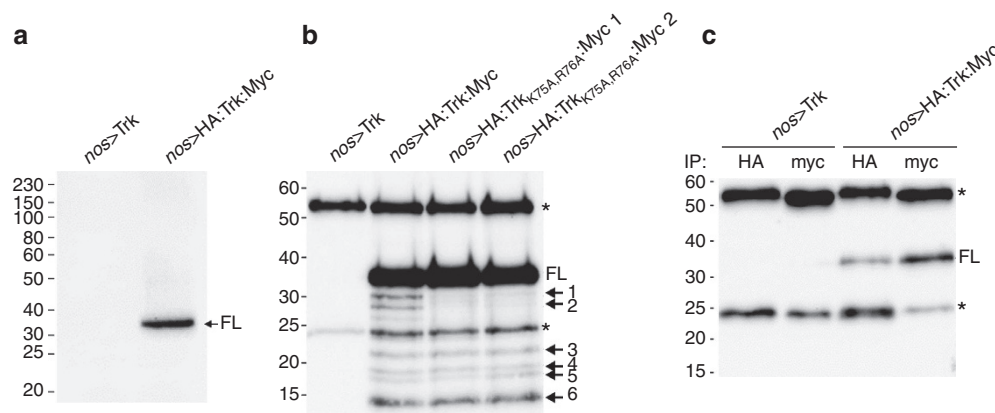


Figure 3 | Trk is cleaved multiple times. (a) Immunoblot without prior immunoprecipitation of protein extracted from embryos expressing HA:Trk:Myc. Only full-length Trk (FL) is detected using anti-Myc. (b) Immunoblot of protein extracts immunoprecipitated (using anti-Myc) from embryos expressing Trk constructs and blotted with anti-Myc. HA:Trk:Myc extracts contain a predominant Trk species (FL = full length) and at least six C-terminal Trk fragments (arrows) not observed in untagged Trk extracts (*nos>Trk*). Two independent Trk_{K75A,R76A} mutants lack fragments 1 and 2. (c) Immunoblot of protein extracts immunoprecipitated (using anti-Myc or anti-HA) from embryos expressing HA:Trk:Myc and blotted with anti-HA. Note that full-length (FL) Trk protein immunoprecipitated with anti-Myc can be detected with anti-HA. No additional N-terminal Trk fragments are observed in extracts immunoprecipitated with anti-HA. * indicates immunoglobulin bands. Images are representative of at least two replicate immunoblots.

Tsl does not influence the observed Trk cleavage pattern. Finally, we sought to test the current model that Tsl is required for Trk cleavage. This was achieved by expressing the HA:Trk:Myc construct in a *tsl*-null mutant background. Unexpectedly, we saw no difference in the Trk cleavage pattern in the absence of Tsl (Fig. 5a). Given that Tor signalling only occurs at the embryo poles, there may be a small amount of Tsl-dependent Trk cleavage product that is below the detection level of our assay. To address this, we ectopically produced Tsl from all ovarian follicle cells using *c355-Gal4* (ref. 15) while also producing tagged Trk from the germline. Unrestricted expression of Tsl results in ubiquitous Tor activation and causes the spliced cuticle phenotype—an expansion of the terminal regions at the expense of central segments (ref. 10 and Fig. 5b). We reasoned that under this scenario, the abundance of a Tsl-dependent Trk cleavage product should be greatly increased. However, we did not observe any additional Trk cleavage products in these embryos (Fig. 5c).

Discussion

Taken together, our data strongly support the idea that Trk must be cleaved in order to bind and activate the Tor receptor. While the Trk cleavage products that we detect are produced independently of Tsl, we cannot completely eliminate the possibility that the localized influence of Tsl on Trk cleavage events is extremely subtle, and lies beyond what we are able to detect. Alternatively, we argue that a simpler explanation for our data is that Tsl acts in terminal patterning after Trk cleavage.

In this latter scenario, if Trk does not require Tsl for proteolytic activation, then how could localized Trk/Tor signalling be achieved? One possibility is that activated Trk requires Tsl for binding to Tor. However, this seems unlikely as Sprenger and Nüsslein-Volhard¹¹ elegantly demonstrated that the Tor ligand can diffuse and activate Tor that is artificially localized to only the middle of the embryo. This cannot require direct participation by Tsl, as Tsl is localized to the embryo poles via its interaction with the vitelline membrane and is not present elsewhere in the embryo¹⁶. Further, we have not been able to detect direct interactions between Trk/Tor/Tsl in co-immunoprecipitation experiments.

We thus propose an alternative hypothesis for the events that surround localized Trk/Tor signalling. Tsl shares no sequence similarity to any known protease family, and instead

is a member of the cholesterol-dependent cytolysin (CDC)/MACPF superfamily^{17,18}. The primary characterized function of this protein superfamily is in pore formation and/or membrane disruption^{18–22}; however, it has not been considered how such a role might relate to localized Trk/Tor signalling. In this regard, it is notable that a general response to membrane damage (including pore-induced lesions) involves local stimulation of both endocytosis and exocytosis as part of the membrane repair response^{23–27}. For example, it has been shown that the pore-forming toxin Streptolysin O (a member of the CDC/MACPF superfamily) induces exocytosis of lysosomes and the release of enzymes required for membrane repair^{28,29}. This may represent an ancient defensive response to pathogen attack^{25,30–32}. Accordingly, given a known role for CDC/MACPF proteins in exocytosis, we suggest that the trafficking machinery required for active Trk secretion may be Tsl dependent.

Methods

Drosophila stocks. The following stocks were used: *hs-FLP hs-I-SceI* (BL6935), *ey-FLP* (BL5580), *w¹¹¹⁸* (BL5905), *Gal4:VP16-nos.UTR* (BL7293), *c355-Gal4* (BL3750), *UAS-*tsl** (ref. 7), *tsl^A*, a null mutant of *torso*-like (ref. 7) and *tor^{XRI}*, a small deficiency uncovering the *torso* locus⁸ (gift from Dr. Jordi Casanova).

Generation of *trk*-null mutants and transgenic lines. The *trk*-null mutant was generated using ends-out gene replacement³³. First, the donor plasmid pW25-*trk* was built by cloning 2.7 Kbp of upstream (F- 5'-AGCAGGCGCGCTTCAGTGTGATTCGGAAGATT-3', R-5'-TACCCGTACGCACTGGGCAATCAACTAATCA-3') and 3.7 Kbp of downstream (F-5'-AGCAGCGGCCGCGAGAAGGGCAGACTGCAAAAC-3', R-5'-TACCCGTACCTTGATTTTGATCACCAGCAGA-3') sequence flanking the *trk* coding region into the appropriate sites in the ends-out transformation vector pW25. For pW25-*trk* and other Trk constructs, transgenics were generated by injection into *w¹¹¹⁸* embryos (BestGene) using standard protocols³⁴. The donor targeting element was mobilized by crossing to *hs-FLP*, *hs-I-SceI* and applying a heat shock for 80 min at 37 °C daily for days 3–5 of development. Mosaic and white-eyed virgins were crossed to *ey-FLP* and stable lines were established from *w+* progeny (~1/6 vials yielded a *w+* individual). Lines were characterized for targeting events via PCR (A-5'-CCAGCTTGGTGTTAAGAGC-3', B-5'-AGCCCACTTGAGTAGCGAAA-3', C-5'-AGACAACGGTGAGTGGTTCC-3', D-5'-CCAAGACAGGTCACAAAGCA-3'). Of the 14 *w+* lines we generated, two had undergone gene replacement. *trk* transcriptional activity was assessed in the mutants by RT-PCR from ovary derived cDNA using primers specific for *trk* (F-5'-TTCTATGCGGACAGTGATGC-3', R-5'-CCAAATCCAGAGCTGCGTA-3') and a control gene *CyclinK* (F-5'-GAGCATCCTTACACCTTCTCCT-3', R-5'-TAATCTCCGGCTCCCACTG-3').

Wild-type, tagged and mutant Trk constructs, were synthesized, mutated (where necessary) and cloned (Genscript) into pUASP³⁵. The N-terminal tags, 3xMyc, 3xHA and TagRFP, were spliced into the Trk sequence between residues

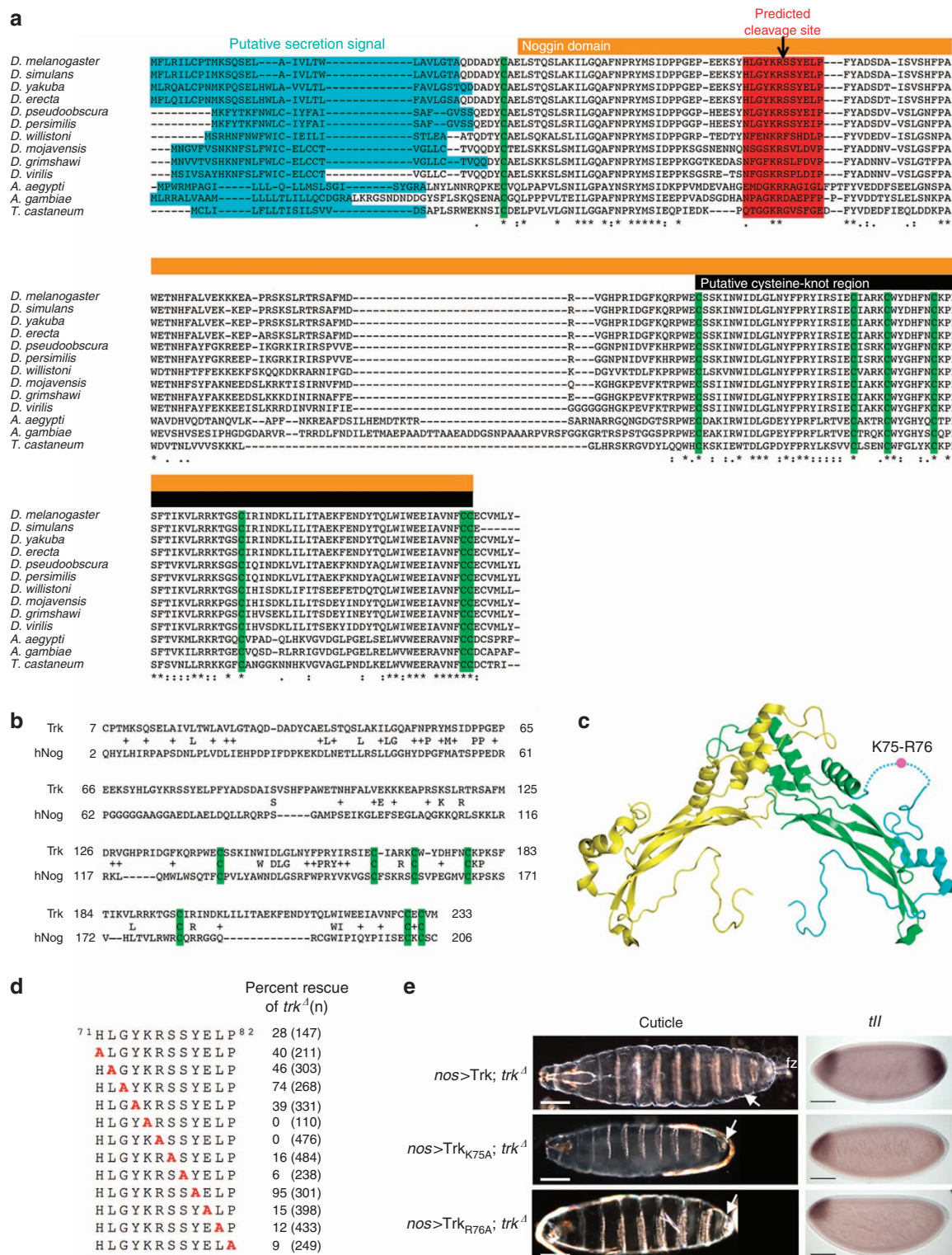


Figure 4 | Cleavage of Trk at K75-R76 is required for terminal patterning. (a) Alignment of insect Trk-like proteins annotated with putative secretion signal (cyan), conserved cysteines (green), predicted cleavage site (arrowed) and surrounding sequence (red). Orange bar indicates a region of significant sequence conservation with the Noggin domain (EXPECT 2.97 $\times 10^{-6}$ for *D. melanogaster*, pfam05806). Black bar denotes the putative cysteine-knot region. (b) Alignment from PSI-BLAST search showing the pairwise match between human Noggin and *D. melanogaster* Trk (EXPECT score 6 $\times 10^{-49}$, where scores below 1 $\times 10^{-6}$ are considered significant³⁷). Conserved cysteine residues that form the 3D cysteine knot structure in Noggin are highlighted in green. (c) X-ray crystal structure of the Noggin dimer² (pdb identifier 1M4U) with constituent monomers in green and yellow. The region equivalent to the Trk N-terminus¹ (mapped using PSI-BLAST alignments) is in cyan on one monomer. K75-R76 in Trk maps to an exposed loop in the N-terminus that is mobile and not visible in electron density (dashed line). Image produced using PyMOL. (d) Alanine scan of putative Trk cleavage site. Twelve constructs, each containing a single-alanine substitution, were tested for rescue of the *trk^d* phenotype (level of rescue is indicated). (e) Rescue was not observed for Trk_{K75A} and Trk_{R76A} mutations; anterior is to the left, maternal genotypes indicated. Scale bars, 100 μ m. For each experiment at least two independent transgenic Trk lines were tested.

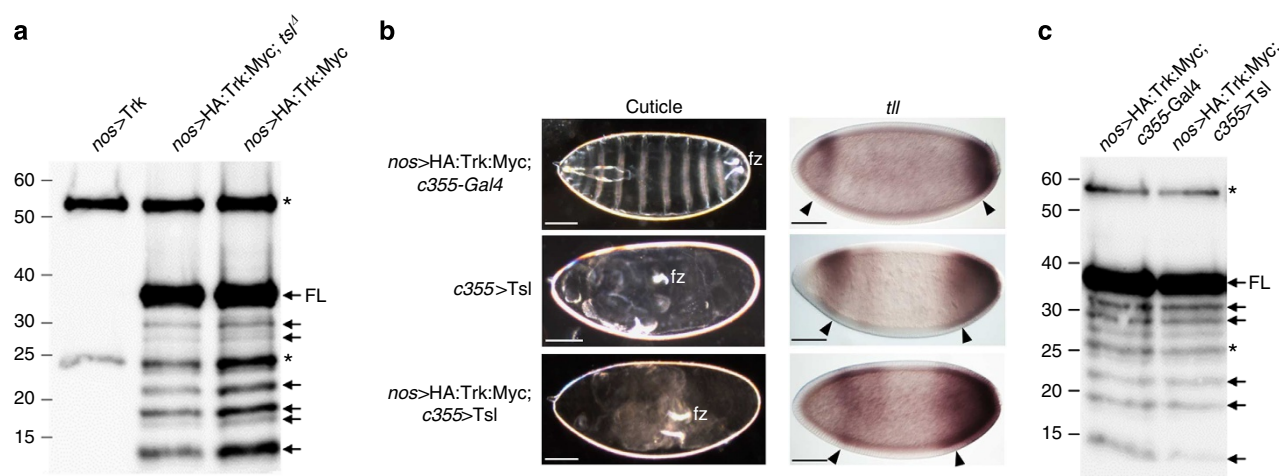


Figure 5 | Trk cleavage occurs independently of Tsl function. (a) Protein was extracted and immunoprecipitated (anti-Myc) from embryos expressing HA:Trk:Myc. Note that all observed C-terminal Trk fragments (arrows) are also present in the absence of Tsl (*tsl*^Δ). (b) Representative cuticles and *tll* in situ hybridizations of embryos laid by mothers of the genotype indicated. Ectopic expression of Tsl using c355-Gal4 results in an un-segmented embryo with a centrally positioned filzkörper (fz) and greatly expanded *tll* domain (arrowed). When HA:Trk:Myc is overexpressed from the germline in this background, the phenotype is unchanged. Anterior is to the left. Scale bars, 100 μm. (c) No additional Trk-cleavage products are observed when Tsl is ectopically expressed. * indicates immunoglobulin bands. FL = full length. Images are representative of at least two repeat experiments.

D34-Y35 and flanked with a short linker peptide (SAGSAS). C-terminal tags (3 × Myc, eGFP) were fused directly to the last residue encoded by the *trk* sequence. For all transgenes, several independent transgenic lines were established and tested.

RNA in situ hybridizations. T7 RNA polymerase (Roche) was used to transcribe a 980 bp fragment of *tll* (F-5'-AGTGCTTTGAGGTCGGAATG-3', R-5'-TTGAGACCTTGTGCATCAGC-3') that had been cloned into pGEM-T easy (Promega) to produce a DIG-labelled antisense RNA probe. In situ hybridization on whole-mount embryos was performed using standard protocols³⁶ before imaging with differential interference contrast optics on a Leica DM LB compound microscope.

Cuticle preparations. Adults were allowed to lay on media containing apple juice supplemented with yeast paste for 24 h before being removed. Embryos were developed for further 24 h before dechoriation in 50% vol/vol bleach and mounting on slides in a mixture of 1:1 Hoyer's solution: lactic acid. Slides were incubated overnight at 65 °C and imaged using dark field optics (Leica).

Protein extraction and immunoprecipitation. Approximately 500 μl volume of 0–6 h-old embryos were homogenized in lysis buffer (50 mM Tris-HCl (pH 7.5), 150 mM NaCl, 2.5 mM EDTA, 0.2% Triton X, 5% glycerol, complete EDTA-free protease inhibitor cocktail (Roche)) and spun at 500g for 5 mins at 4 °C. The supernatants obtained were made up to 1 ml with lysis buffer and incubated with 2 μl anti-Myc (Cell Signalling, 9B11) or 6 μl anti-HA (Roche, 12CA5) overnight at 4 °C. Protein A sepharose beads (100 μl, GE Healthcare; CL-4B) in lysis buffer were added and extracts were incubated for another 4 h. The beads were collected by centrifugation, washed four times with lysis buffer and bound protein was removed via boiling in 40 μl sample buffer containing 6 M urea. Equal amounts of protein were separated by SDS-PAGE (12%) and transferred onto Immobilon-P membrane (Millipore). Membranes were probed with 1:1,000 anti-Myc (Cell Signalling; 9B11) or 1:1,000 anti-HA (Roche, 12CA5), washed and incubated with HRP-conjugated secondary antibody (1:10,000, Southern Biotech). Immunoblots were developed using ECL (GE healthcare) and imaged using a chemiluminescence detector (Vilber Lourmat).

Bioinformatics. The alignment of Noggin and Trunk was produced using the results of PSI-BLAST searches³⁷ using a significance cut-off of 1×10^{-6} in the first 20 interactions³⁸. The structure of Noggin was obtained from the pdb (1M4U, chain A), and Figure 4c produced using PYMOL (Schrödinger, LLC.) Trunk-like protein sequences from various insect species were taken from OrthoDB³⁹ and aligned using Clustal Omega⁴⁰. The alignment was manually adjusted to correct for obvious misalignments and to reflect structural insights derived from 1M4U and other cysteine-knot proteins. SignalP 4.0 (ref. 41) was used to annotate putative secretion signals and the Conserved Domains Database⁴² for determining regions of Trk bearing the Noggin domain.

References

- Duncan, E. J., Benton, M. A. & Dearden, P. K. Canonical terminal patterning is an evolutionary novelty. *Dev. Biol.* **377**, 245–261 (2013).
- Groppe, J. *et al.* Structural basis of BMP signalling inhibition by the cysteine knot protein Noggin. *Nature* **420**, 636–642 (2002).
- Hu, X. D., Yagi, Y., Tanji, T., Zhou, S. L. & Ip, Y. T. Multimerization and interaction of Toll and Spatzle in *Drosophila*. *Proc. Natl Acad. Sci. USA* **101**, 9369–9374 (2004).
- Reeves, G. T. & Stathopoulos, A. Graded dorsal and differential gene regulation in the *Drosophila* embryo. *Cold Spring Harb. Perspect. Biol.* **1**, a000836 (2009).
- Casanova, J., Furriols, M., McCormick, C. A. & Struhl, G. Similarities between Trunk and Spatzle, putative extracellular ligands specifying body pattern in *Drosophila*. *Genes Dev.* **9**, 2539–2544 (1995).
- Casali, A. & Casanova, J. The spatial control of Torso RTK activation: a C-terminal fragment of the Trunk protein acts as a signal for Torso receptor in the *Drosophila* embryo. *Development* **128**, 1709–1715 (2001).
- Johnson, T. K. *et al.* Torso-like functions independently of Torso to regulate *Drosophila* growth and developmental timing. *Proc. Natl Acad. Sci. USA* **110**, 14688–14692 (2013).
- Sprenger, F., Stevens, L. M. & Nüsslein-Volhard, C. The *Drosophila* gene *torso* encodes a putative receptor tyrosine kinase. *Nature* **338**, 478–482 (1989).
- Klinger, M., Erdelyi, M., Szabad, J. & Nüsslein-Volhard, C. Function of *torso* in determining the terminal anlagen of the *Drosophila* embryo. *Nature* **335**, 275–277 (1988).
- Savant-Bhonsale, S. & Montell, D. J. Torso-like encodes the localized determinant of *Drosophila* terminal pattern formation. *Genes Dev.* **7**, 2548–2555 (1993).
- Sprenger, F. & Nüsslein-Volhard, C. Torso receptor activity is regulated by a diffusible ligand produced at the extracellular terminal regions of the *Drosophila* egg. *Cell* **71**, 987–1001 (1992).
- Martin, J. R., Raibaud, A. & Olo, R. Terminal pattern elements in *Drosophila* embryo induced by the torso-like protein. *Nature* **367**, 741–745 (1994).
- Stevens, L. M., Frohnhofer, H. G., Klinger, M. & Nüsslein-Volhard, C. Localised requirement for torso-like expression in follicle cells for development of terminal anlagen of the *Drosophila* embryo. *Nature* **346**, 660–663 (1990).
- Morisato, D. & Anderson, K. V. Signalling pathways that establish the dorsal-ventral pattern of the *Drosophila* embryo. *Annu. Rev. Genet.* **29**, 371–399 (1995).
- Hrdlicka, L. *et al.* Analysis of twenty-four Gal4 lines in *Drosophila melanogaster*. *Genesis* **34**, 51–57 (2002).
- Stevens, L. M., Beuchle, D., Jurcsak, J., Tong, X. & Stein, D. The *Drosophila* embryonic patterning determinant torso-like is a component of the eggshell. *Curr. Biol.* **13**, 1058–1063 (2003).
- Ponting, C. P. Chlamydial homologues of the MACPF (MAC/perforin) domain. *Curr. Biol.* **9**, R911–R913 (1999).
- Rosado, C. J. *et al.* A common fold mediates vertebrate defense and bacterial attack. *Science* **317**, 1548–1551 (2007).

19. Hadders, M. A., Beringer, D. X. & Gros, P. Structure of C8alpha-MACPF reveals mechanism of membrane attack in complement immune defense. *Science* **317**, 1552–1554 (2007).
20. Kondos, S. C. *et al.* The structure and function of mammalian membrane-attack complex/perforin-like proteins. *Tissue Antigens* **76**, 341–351 (2010).
21. Law, R. H. *et al.* The structural basis for membrane binding and pore formation by lymphocyte perforin. *Nature* **468**, 447–451 (2010).
22. Rosado, C. J. *et al.* The MACPF/CDC family of pore-forming toxins. *Cell Microbiol.* **10**, 1765–1774 (2008).
23. Idone, V., Tam, C. & Andrews, N. W. Two-way traffic on the road to plasma membrane repair. *Trends Cell Biol.* **11**, 552–559 (2008).
24. Medina, D. L. *et al.* Transcriptional activation of lysosomal exocytosis promotes cellular clearance. *Dev. Cell.* **21**, 421–430 (2011).
25. Reddy, A., Caler, E. V. & Andrews, N. W. Plasma membrane repair is mediated by Ca(2+)-regulated exocytosis of lysosomes. *Cell* **106**, 159–169 (2001).
26. Rodriguez, A., Webster, P., Ortego, J. & Andrews, N. W. Lysosomes behave as Ca²⁺-regulated exocytic vesicles in fibroblasts and epithelial cells. *J. Cell Biol.* **137**, 93–104 (1997).
27. Tam, C. *et al.* Exocytosis of acid sphingomyelinase by wounded cells promotes endocytosis and plasma membrane repair. *J. Cell Biol.* **189**, 1027–1038 (2010).
28. Corrotte, M., Fernandes, M. C., Tam, C. & Andrews, N. W. Toxin pores endocytosed during plasma membrane repair traffic into the lumen of MVBs for degradation. *Traffic* **13**, 483–494 (2012).
29. Corrotte, M. *et al.* Caveolae internalization repairs wounded cells and muscle fibers. *Elife* **2**, e00926 (2013).
30. McNeil, P. L. & Steinhardt, R. A. Loss, restoration and maintenance of plasma membrane integrity. *J. Cell Biol.* **137**, 1–4 (1997).
31. McNeil, P. L. & Terasaki, M. Coping with the inevitable: how cells repair a torn surface. *Nat. Cell Biol.* **3**, E124–E129 (2001).
32. Husmann, M. *et al.* Elimination of a bacterial pore-forming toxin by sequential endocytosis and exocytosis. *FEBS Lett.* **583**, 337–344 (2009).
33. Gong, W. J. & Golic, K. G. Ends-out, or replacement, gene targeting in *Drosophila*. *Proc. Natl Acad. Sci. USA* **100**, 2556–2561 (2003).
34. Rubin, G. M. & Spradling, A. C. Vectors for P element-mediated gene transfer in *Drosophila*. *Nucleic Acids Res.* **11**, 6341–6351 (1983).
35. Rorth, P. Gal4 in the *Drosophila* female germline. *Mech. Dev.* **70**, 111–118 (1998).
36. Tomancak, P. *et al.* Systematic determination of patterns of gene expression during *Drosophila* embryogenesis. *Genome Biol.* **3**, doi:10.1186/gb-2002-3-12-research0088 (2002).
37. Altschul, S. F. *et al.* Gapped BLAST and PSI-BLAST: a new generation of protein database search programs. *Nucl. Acids Res.* **25**, 3389–3402 (1997).
38. Park, J. *et al.* Sequence comparisons using multiple sequences detect three times as many remote homologues as pair-wise methods. *J. Mol. Biol.* **284**, 1201–1210 (1998).
39. Waterhouse, R. M., Tegenfeldt, F., Zdobnov, E. M. & Kriventseva, E. V. OrthoDB: a hierarchical catalog of animal, fungal and bacterial orthologs. *Nucl. Acids Res.* **41**, D358–D365 (2013).
40. Sievers, F. *et al.* Fast, scalable generation of high-quality protein multiple sequence alignments using Clustal Omega. *Mol. Syst. Biol.* **7**, 539 (2011).
41. Petersen, T. N., Brunak, S., von Heijne, G. & Nielsen, H. Signal P4.0: discriminating signal peptides from transmembrane regions. *Nat. Methods* **8**, 785–786 (2011).
42. Marchler-Bauer, A. *et al.* CDD: conserved domains and protein three-dimensional structure. *Nucl. Acids Res.* **41**, D348–D352 (2013).

Acknowledgements

We thank Karyn Foote and the Australian *Drosophila* Biomedical Research Facility (OzDros) for technical support and Anabel Herr, Richard Burke and Marc Freeman for valuable discussions. This work was supported by an Australian Research Council (ARC) grant to J.C.W. and C.G.W. J.C.W. is a National Health and Medical Research Council Senior Principal Research Fellow. J.C.W. further acknowledges the support of an ARC Federation Fellowship. We acknowledge the support of the Monash platforms, in particular Monash Micro Imaging (MMI) and the Monash Biomedical Proteomics Facility.

Author contributions

C.G.W. and J.C.W. conceived the experiments, interpreted the data and co-led the work. M.A.H. and T.K.J. performed the experiments. All authors wrote the manuscript.

Additional information

Competing financial interests: The authors declare no competing financial interests.

Reprints and permission information is available online at <http://www.npg.nature.com/reprintsandpermissions/>

How to cite this article: Henstridge, M. A. *et al.* Trunk cleavage is essential for *Drosophila* terminal patterning and can occur independently of Torso-like. *Nat. Commun.* 5:3419 doi: 10.1038/ncomms4419 (2014).